Cytokine gene expression and molecular detection of *Mycobacterium avium* subspecies *paratuberculosis* in organs of experimentally infected mice[1]

David G.G. Schwarz[2], Pricila A.G. Pietralonga[2], Marina C.C. Souza[2], Isabel A. Carvalho[2], Rosyane S. Cruzeiro[3], Juaci V. Malaquias[4], Laércio A. Benjamin[2], Abelardo Silva Júnior[2] and Maria A.S. Moreira[2]*

ABSTRACT.- Schwarz D.G.G., Pietralonga P.A.G., Souza M.C.C., Carvalho I.A., Cruzeiro R.S., Malaquias J.V., Benjamin L.A., Silva Júnior A. & Moreira M.A.S. 2015. **Cytokine gene expression and molecular detection of *Mycobacterium avium* subspecies *paratuberculosis* in organs of experimentally infected mice.** *Pesquisa Veterinária Brasileira 35(5):396-402.* Departamento de Veterinária, Universidade Federal de Viçosa, Av. Peter Henry Rolfs s/n, Viçosa, MG 36570-900, Brazil. E-mail: masm@ufv.br

Mycobacterium avium subspecies *paratuberculosis* (MAP) can infect ruminants and remain subclinical for long periods within herds. The identification of organs that are more susceptible to infection and the evaluation of cytokine expression at the site of infection are important to understand the pathogenesis of MAP. In this study, the probability of detection of MAP-DNA and the expression of cytokines in organs of C57BL/6 mice infected intraperitoneally for 120 days were evaluated. Among the evaluated organs, the spleen (85%), colon (75%) and liver (60%) had the highest frequency of positivity. When compared these frequencies between organs, it has been found that the spleen had 1.54 times as likely to be positive in relation to the ileum, and 2.0 times more likely in relation to the Peyer's patches. In addition, at 60 days post-infection, the spleen and the liver were responsible for upregulation of IFN-γ, and the ileum by TNF-α and IL-4. The results indicate that the spleen is the best organ for evaluating an experimental infection by MAP, especially in the initial stages of the infection. Moreover, it showed that the spleen, liver and ileum have a direct role in the inflammatory response in experimental models.

INDEX TERMS: *Mycobacterium avium* subsp. *paratuberculosis,* mice, Johne's disease, IS*900*, experimental infection.

RESUMO.- [**Expressão de citocinas e detecção molecular de *Mycobacterium avium* subspecies *paratuberculosis* em órgãos de camundongos infectados experimentalmente.**] *Mycobacterium avium* subespécie *paratuberculosis* (MAP) pode infectar ruminantes e permanecer subclínica por longos períodos nos rebanhos. A identificação de órgãos mais susceptíveis à infecção e a avaliação da expressão das citocinas no local da infecção são importantes para

Contribution of the Authors:

Schwarz D.G.G. collected the samples, performed the molecular analysis (nested PCR), analyzed the data and wrote the manuscript;

Pietralonga A.G.P. participated in the sample collection, molecular analysis and interpretation of the results (real time qPCR);

Souza M.C.C. and Carvalho I.A. participated in the sample collection, molecular analysis and classic microbiology (nested-PCR and MAP cultivation);

Cruzeiro R.S. and Benjamin L.A. participated in the tissue preparation and histological analysis;

Malaquias J.V. gave assistance to the statistical analysis and experimental delineation;

Silva Júnior A. contributed to the experimental molecular delineation (nested-PCR and real time qPCR); Moreira M.A.S. coordinated all activities, oriented dissertations of the first two authors (the partial results of which will be submitted also to this journal), and revised the experimental part of this paper and the data obtained.

compreender a patogênese de MAP. Neste estudo foi avaliada a probabilidade de detecção de DNA de MAP e a expressão de citocinas em órgãos de camundongos C57BL/6 infectados por via intraperitoneal durante 120 dias. Dentre os órgãos avaliados, o baço (85%), cólon (75%) e fígado (60%) tiveram as maiores frequências de positividade. Quando comparadas essas frequências entre os órgãos, verificou-se que o baço teve 1,54 vezes mais probabilidade de ser positivo em relação ao íleo, e 2,0 vezes mais probabilidade em relação às placas de Peyer. Além disso, aos 60 dias pós infecção, o baço e o fígado foram responsáveis pela maior expressão de IFN-γ e o íleo pela TNF-α e IL-4. Os resultados indicam que o baço é o melhor órgão para avaliar uma infecção experimental por MAP, principalmente nos períodos iniciais da infecção. Além disso, demonstrou que o baço, fígado e íleo têm importância direta na resposta inflamatória de modelos experimentais.

TERMOS DE INDEXAÇÃO: *Mycobacterium avium* subsp. *paratuberculosis,* doença de Johne, IS*900*, murinos, infecção experimental.

INTRODUCTION

Mycobacterium avium subspecies *paratuberculosis* (MAP) is the etiologic agent of paratuberculosis also known as Johne's disease. It is a chronic granulomatous enteritis with clinically progressive diarrhea, emaciation and death that mainly affects domestic and wild ruminants (Chiodini et al. 1984, Clarke 1997). In addition, MAP is important for public health due to its possible relationship with Crohn's disease (Mendoza et al. 2009). Although ruminants are the main natural hosts of MAP, and thus better models for testing, they need to be maintained in evaluation for long periods before clinical manifestation, limiting these animals models only to the few institutions with facilities capable of meeting these needs (Harris & Barletta 2001). For these reasons, different strains of mice have been used in studies related to infection by MAP, having low cost, easy handling and short experimentation time (Mutwiri et al. 1992, Chiodini & Buergelt 1993, Roupie et al. 2008).

In experimental infections in cattle, MAP had a predilection for involving parts of the ileum including the ileocecal valve, jejunum and corresponding lymph nodes, maintaining the infection in these tissues (Sweeney et al. 2006, Stabel et al. 2009). Still, the recovery of viable MAP in extra-intestinal tissues such as the spleen and tonsils was possible by experimental infection with high doses of oral inoculums (Sweeney et al. 2006). However, the evaluation of experimental hematogenous dissemination of MAP in various tissues of sheep, reinforced the assertion of the disease's predilection for infection in filtering organs, the spleen, lungs and liver instead of gut-associated tissues, as occurs with systemic involvement (Bower et al. 2013). These patterns of MAP tissue disseminations must also be evaluated in mice, in order to establish a better comparison among these experimental models with ruminants. Furthermore, it is very important to associate this information with the inflammatory potential of the agent, mainly evaluating the ability of this agent to stimulate cytokine expression in these tissues.

Pro-inflammatory cytokines such as IFN-γ, IL-2 and TNF-α are critical for the recruitment of immune cells to combat the infection; however, the prolonged activation of cytokines can trigger a sequence of events that can result in damage to the tissue and lesion formation at sites of infection (Clarke 1997). Possibly in response to damage caused by pro-inflammatory cytokines, anti-inflammatory cytokines, such as IL-10, are developed to monitor local tissue damage and immune responses in infection sites (Coussens et al. 2004). The immune response at the site of infection is poorly defined and in this sense, the comparison of cytokine expression in the peripheral blood can be different during the course of paratuberculosis, because it is influenced by the phases of infection (Lee et al. 2001, Coussens et al. 2004, Tanaka et al. 2005). Studies often evaluate the immune response in a peripheral blood (Coussens et al. 2002, Coussens et al. 2004, Koo et al. 2004), but there is little information about the contribution of the immune response in specific organs during MAP infection.

The aim of this study was to evaluate the detection probability of MAP and the expression of specific cytokines in C57BL/6 mice tissues at different times after intraperitoneal inoculation (IP).

MATERIALS AND METHODS

Animals*.* The experiment was conducted using 28 female C57BL/6 mice (Universidade Federal de Viçosa, Brazil), between six and eight weeks old, weighing 18-20g. Animals were maintained in a laboratory for animal infection with free access to water and feed. The protocol for animal experimentation was approved by the Ethics Committee on Animal Use of the Universidade Federal de Viçosa, Brazil (Protocol number CEUA, 92/2011), and the experimental procedures were performed according to NIH Guide for the Care and Use of Laboratory Animals.

Bacterial strain. A bovine strain designated MAP66115-98, kindly provided by Dr. Yung-Fu Chang, from Cornell University--USA, was used to challenge the mice. This strain was grown in Middlebrook 7H9 broth supplemented with oleic acid-albumin-dextrose-catalase (OADC) (10% vol/vol) with 2 mg/L of mycobactin *J* (Allied Monitor, Inc. Fayette, MO) at a temperature of 37°C. After six weeks of cultivation, the microorganism was quantified using the comparative method of tubes from the nephelometric scale of McFarland (Verna et al. 2007) corresponding to a turbidity equivalent to 1.0 McFarland standard and confirmed by optical density at 600 nm (OD_{600}=0.1) with a Biomate 3 spectrophotometer (Thermo Scientific Corporation). Then, the culture was centrifuged for 5 minutes at 14000 x *g*, and the pellet was washed twice in phosphate-buffered saline (PBS, pH 7.2) and suspended in a concentration of 3×10^8 CFU/mL. To induce an infection in mice, this suspension was then diluted 1:4 to reach a concentration of 7.5×10^7 CFU/mL and used to challenge the mice. To verify the inoculum viability, aliquots were incubated in tubes with Herrold egg yolk media (HEYM) with mycobactin *J* at 37°C for 16 weeks. Colonies grown were confirmed by conventional PCR using IS*900* according to Sivakumar et al. (2005). IS*900* is an insertion element generally accepted as the standard marker for MAP and being a very well-conserved sequence is a target for MAP molecular diagnosis (Carvalho et al. 2012).

Inoculation of mice. The mice were splitted into two groups. In group I, 20 animals were inoculated with 250 µL of inoculum containing the MAP66115-98 strain at a concentration of 7.5×10^7 CFU/mL, and in group II, eight animals were inoculated with 250

μL of autoclaved PBS. Inoculations were performed by IP injection in the right lower quadrant of the abdomen. At 30, 60, 90 and 120 days post-inoculation, five animals in group I and two animals in group II were randomly selected and euthanized by administering sodium thiopental at a dose of 100mg/kg via IP injection. Immediately, animals were necropsied, and the liver, spleen, terminal ileum, colon and Peyer's patches were collected aseptically and fragments were stored for molecular and histopatological analyzes.

IS*900* nested-PCR. Tissues were grinded with a pestle. The DNA extraction was performed with a Wizard® Genomic DNA Purification Kit (Promega, Madison, WI), according to the manufacturer's instructions. Results of extraction were verified by electrophoresis in 1% agarose gels (Invitrogen, Washington, DC) in Tris-Borate-EDTA (TBE) buffer, stained with GelRed™ (Biotium Inc., CA), and visualized by ultraviolet light (UV).

The *nested*-PCR was performed according to Englund et al. (1999), with modifications. Different primer pairs were used to amplify 563 bp in the first reaction and 210 bp in the second reaction (Englund et al. 1999) (Table 1). For the reaction, Go Taq® Green Master-Mix Kit (2X) (Promega) was used, following the manufacturer's protocol for a 25μl reaction volume. Final concentration of the DNA template was 200hg/μL and 10μM of each primer (*forward and reverse*). The following program was used: 94°C for 3 min, 35 cycles of 94°C for 1 min, 63°C for 1 min, 72°C for 1 min, and a final extension of 72°C for 5 min. For the second reaction were used the same concentrations as the first reaction, but 1μL of the first reaction product was used. The second reaction parameters were similar to the first.

The result was verified by electrophoresis in 1% agarose gels (Invitrogen, Washington, DC, USA) in Tris-Borate-EDTA (TBE), stained with GelRed™ (Biotium Inc., CA) diluted 1:500, and visualized using an Eagle Eye II UV transluminator (Stratagene, La Jolla, CA, USA).

For the PCR positive and negative controls, the MAP K-10 strain and ultrapure water were used, respectively. For the negative control of the experiment, the DNA of organs from animals inoculated with PBS was used. The molecular weight and size marker was the 100-bp DNA Ladder (Promega, Madison, WI).

Real Time PCR. Real-Time Quantitative Reverse Transcription PCR (qRT-PCR) was performed to determine the expression levels of the pro-inflammatory IL-2, IFN-γ, and TNF-α and the anti-inflammatory IL-4 and IL-10 cytokines target genes relative to *β*-actin, the endogenous control. For this, 0,5g of organs were homogenized, gently mixed with 750μL of TRIzol® Reagent (Life Technologies) and maintained at room temperature for 5 min. RNA was extracted according to the manufacturer's instructions (Life Technologies, Grand Island, USA) and was later treated with DEPC-treated water (Life Technologies, Grand Island, USA) at 37°C for 10 minutes. Total RNA quantification was performed by the fluorescence method (Qubit® 2.0 Fluorometer) according to the manufacturer's instructions, and RNA integrity was confirmed by visualization of the fragments in agarose gel electrophoresis with 0.8% (Invitrogen, Washington, DC) in TBE buffer and visualized by UV incidence. cDNA synthesis was performed using M-MLV Reverse Transcriptase (Invitrogen, Washington, DC) according to the manufacturer's specifications. qRT-PCR of selected genes (Table 1) was conducted using a Maxima SYBR® Green/ROX qPCR Master Mix kit (2X) (Fermentas, Maryland, USA) and a Eco™ Real-Time PCR System (Illumina Inc., São Paulo, Brazil). The following program was used: 50°C for 2 min, 95°C for 10 min, 95°C for 15 s, and 60°C for 1 min for 40 cycles. The reactions were performed simultaneously for the target genes and the endogenous control. The Ct mean values were obtained from duplicate reactions and used to calculate the relative gene expression of target genes by the comparative method using the $2^{-\Delta\Delta Ct}$ formula (Livak & Schmittgen 2001).

Histopathology. The organ portions were fixed in 4% paraformaldehyde and embedded in paraffin (Paraplast plus®, Sigma). Two slides were made for each organ, one for hematoxylin and eosin (HE) and another for Ziehl-Neelsen (ZN) staining, using standard staining methodology. A Reichert-Jung 2045 microtome (Multicut, Germany) was used to obtain serial sections with a thickness of 3 μm, where four sections were prepared for each histological slide.

Statistical analysis. The differences in the frequency were analyzed by Pearson's chi-square (χ^2) test ($p<0.05$) and the strength of association by Cramer's "V" test using the Statistical Package for the Social Sciences (SPSS) software version 19.0 for Windows (IBM SPSS Inc, Chicago, USA). To verify the probability of positivity of a specific organ relative to time post-inoculation, the conditional probability (CP) analysis was used according to the formula below, where A is the positive number of an organ "x" in a specific day of the experimental infection and B is the positive sum for all days of experimental infection in this organ:

$$CP = (A_x / B_x) \times 100$$

For the evaluation of the measure of association between two different organs, the relative risk (RR) was used with respective

Table 1. Oligonucleotides used in quantitative real-time RT-PCR and *nested*-PCR techniques

Genes		Sequence of oligonucleotides (5'-3')	base pairs (bp)	Reference
IL-2	F	TCCAGAACATGCCGCAGAG	141	Chen et al. (2008)
	R	CCTGAGCAGGATGGAGAATTACA		
IL-4	F	CTGACGGCACAGAGCTATTGA	216	Park et al. (2008)
	R	TATGCGAAGCACCTTGGAAGC		
IL-10	F	CAATAACTGCACCCACTTCCC	310	Park et al. (2008)
	R	GAGAAATCGATGACAGCGCCT		
INF-γ	F	CTGACGGCACAGAGCTATTGA	92	Park et al. (2008)
	R	TATGCGAAGCACCTTGGAAGC		
TNF-α	F	TGGGAGTAGACAAGGTACAACCC	175	Chen et al. (2008)
	R	CATCTTCTCAAAATTCGAGTGACAA		
β-actina	F	TAAAACGCAGCTCAGTAACAGTCCG	349	Yao et al. (2010)
	R	TGGAATCCTGTGGCATCCATGAAAC		
s204ᵃ	F	TGATCTGGACAATGACGGTTACGGA	563	Englund et al. (1999)
s749ᵃ	R	CGCGGCACGGCTCTTGTT		
s347ᵃ	F	GCCGCGCTGCTGGAGTTGA	210	Englund et al. (1999)
s535ᵃ	R	AGCGTCTTTGGCGTCGGTCTTG		

[a] Primers used in *IS900 nested*-PCR.

confidence intervals for a significance level of 5%, according to the formula below, where "a" is the positive number of an organ "x", b is the negative number of an organ "x", c is the positive number of an organ "y", and d is the negative number of an organ "y":

$$RR = (a_x/(a_x+b_x)) / (c_y/(c_y+d_y))$$

The construction of graphs and tables were formatted in Excel 2007 software (Microsoft, USA). Quantitative data were obtained using the GraphPad Prism Software version 5 (GraphPad Software, Inc.) and compared using analysis of variance ANOVA with Bonferroni's multiple comparison test as a post test (p<0.05).

RESULTS

MAP detection, positive organ proportion and probability

Amplifications of 210-bp fragments from IS*900 nested*-PCR were observed in 64.9% (61/94) of the collected samples. The spleen showed more positives 27.8% (17/61), followed by the colon 24.6% (15/61), liver 19.7% (12/61), terminal ileum 18.0% (11/61), and Peyer's patches 9.8% (6/61). At least two organs of each mouse were positive for each of the inoculation times (Fig.1).

The proportion of positive results by each group of organs, regardless of post-inoculation period, showed a variation in the frequency, where the spleen had 85% positivity, followed by colon (75%), liver (60%), terminal ileum (55%) and Peyer´s patches (43%). The first three positive organ-proportion were statistically significant (p<0.05) and had an average size association effect by Cramer's "V" test .

In Table 2, the proportion of positive organs and the conditional probability for all days post-inoculation is shown. The highest probability of the liver being positive occurred at 30 and 90 days with 33.3% (4/12). However, for the spleen, the probability of being positive at 30 days was the lowest of all other organs at 11.8% (2/17). But, after 60 days, this probability had stabilized at 29.4% (5/17) through the 120 days of the experiment. For the colon, the highest probability of being positive occurred at 30 days post-inoculation at 33.3% (5/15), which was the same percentage that the liver (33.3%), and the lowest at 90 days was 13.3% (2/15). When the ileum was analyzed, it showed 36.4% (4/11) positives at 120 days post-inoculation and 18.2% (2/11) at 30 and 60 days, respectively. In the case of Peyer's patches, the probability of being positive after 60 days was almost the same during subsequent periods, at 33.3% (2/6).
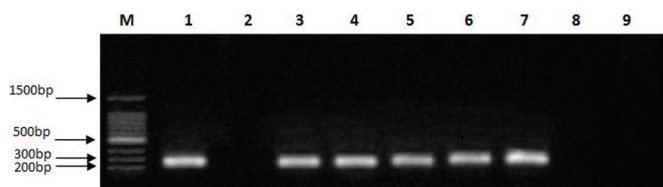

Fig.1. Products of *nested*-PCR in 1% agarose gel (210bp). (M) molecular size marker 100bp-DNA Ladder; (1) positive control: K-10;(2) negative control - ultrapure water; (3), (4), (5), (6) and (7) amplified samples of liver, spleen, colon, ileum Peyer's patch, respectively, after 120 days pos-infection by strain MAP66115-98; (8)and (9) - samples from control animals (inoculated with phosphate-buffered saline).

Table 2. Proportions and probabilities of the organs. Proportion of positives and conditional probability in relation to time post-inoculation of different organs of C57BL/6 mice inoculated IP with 7.5x10⁷CFU/mL of the MAP66115-98 strain

Organs	Post-inoculation time (days)	Number of samples		Proportion of positive organs	Conditional probability (%)
		Positive	Negative		
Liver	30	5/4	5/1	0.8	33.3
	60	5/2	5/3	0.4	16.7
	90	5/4	5/1	0.8	33.3
	120	5/2	5/3	0.4	16.7
Spleen	30	5/2	5/3	0.4	11.8
	60	5/5	5/0	1.0	29.4
	90	5/5	5/0	1.0	29.4
	120	5/5	5/0	1.0	29.4
Colon	30	5/5	5/0	1.0	33.3
	60	5/4	5/1	0.8	26.7
	90	5/2	5/3	0.4	13.3
	120	5/4	5/1	0.8	26.7
Ileum	30	5/2	5/3	0.4	18.2
	60	5/3	5/2	0.6	27.3
	90	5/2	5/3	0.4	18.2
	120	5/4	5/1	0.8	36.4
Peyer's patches	30	nda[a]	nda	nda	0.0
	60	5/2	5/3	0.4	33.3
	90	5/2	5/3	0.4	33.3
	120	4/2	4/2	0.5	33.3

[a] = samples not determined 30 days post-inoculation.

Table 3. Relationship between organs with relative probability above 1.00 and the confidence intervals (CI) at 95% significance

Relationship between organs	Relative Risk (RR)	CI (95%)
Liver *vs* ileum	1.09	0.64 – 1.86
Liver *vs* Peyer's patches	1.40	0.72 – 2.73
Spleen *vs* liver	1.40	0.95 – 2.08
Spleen *vs* colon	1.13	0.83 – 1.55
Spleen *vs* ileum[a]	1.54	1.02 – 2.33
Spleen *vs* Peyer's patches[a]	2.00	1.18 – 3.33
Colon *vs* liver	1.25	0.81 – 1.93
Colon *vs* ileum	1.37	0.86 – 2.16
Colon *vs* Peyer's patches	1.74	0.98 – 3.12
Ileum *vs* Peyer's patches	1.27	0.64 – 2.59

[a] Significant associations (p<0.05).

Association measures-organ assessments

The positive associations between organs that had an RR above 1.00 are presented in Table 3. Among all associations, the spleen/ileum and spleen/Peyer's patches were statistically significant (p<0.05). Thus, the spleen was 1.54 times more likely to be positive compared to ileum and 2.00 times more likely than Peyer's patches.

Quantitative expression of pro and anti-inflammatory cytokines

Expression of pro-inflammatory and the anti-inflammatory cytokine were verified in most tissues of infected mice when compared to controls. However, significant upregulation was detected mainly at 60 days after challenge. During this period, the expression of IFN-γ in liver was significantly higher (p<0.05) compared to the 90 and 120 days pos-challenged, and to the negative control (Fig.2A). Moreover, the expression of IFN-γ in the spleen was signi-
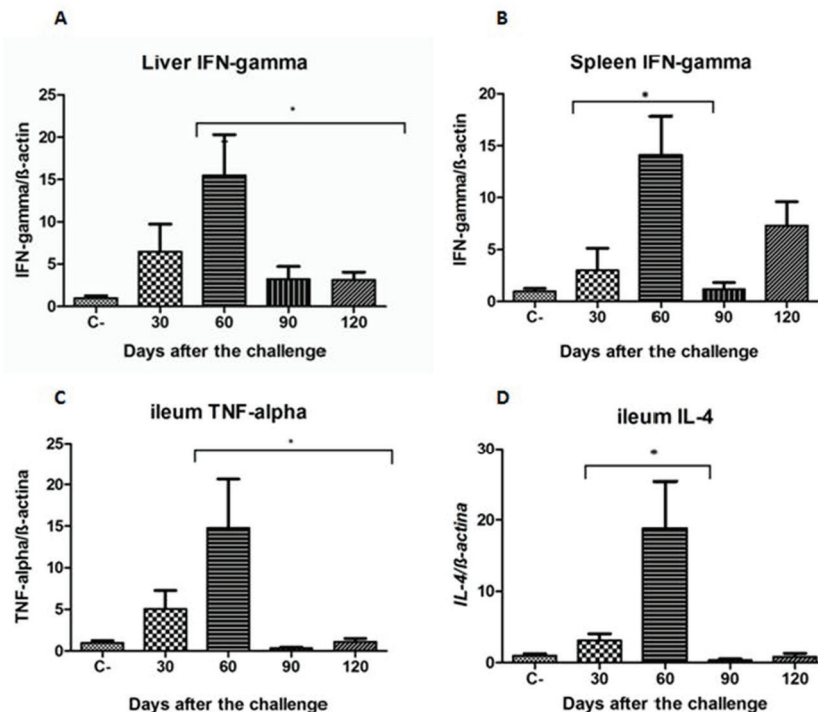
Fig.2. Expression of mRNA in organs. Relative expression of RNA transcripts of pro and anti-inflammatory cytokines that showed statistical significance of 5% (*) in organs of C57BL/6 mice challenged with the MAP66115-98 strain in relation to days post-inoculation. (**A**) mRNA of IFN-γ in the liver; (**B**) mRNA of IFN-γ in the spleen; (**C**) mRNA of TNF-α in the ileum; and (**D**) mRNA of IL-4 in the ileum.

ficant (p<0.05) for only the 30 days post infection (Fig.2B). In the ileum, the expression of IL-4 at 60 days was significantly higher (p<0.05) compared to the values obtained at 30 days and for TNF-α, the significantly differences were verify when compared to the 90, 120 days pos-challenged and to the negative control (Fig.2C,D).

Colon and Peyer's patches had no significant differences, but there were important expression values. In the colon, the highest values expressed were IL-10 (6.58 times higher) and TNF-α (10.48 times higher) at 60 and 90 days, respectively. In the same periods IL-4 (5.43 and 7.02 times, respectively) had the highest levels of expression in the Peyer's patches (data not shown).

Histopathology analysis

Analysis of organ sections not revealed significant findings on histological examination or acid-fast bacilli visualization.

DISCUSSION

This study allowed establishing a parameter detection of MAP-DNA in organs of C57BL/6 mice experimentally infected via IP and evaluated the contribution of these organs in the expression of pro and anti-inflammatory cytokines during MAP infection.

Although it was possible to detect the microorganisms in different organs, it was not possible to see any gross morphological or histological lesions. MAP is often associated with tissue damage and clinical manifestations, but the agent can also colonize tissues and establish infection, even

not correlated with microscopic lesions (Stabel et al. 2009, Allen et al. 2011).

Spleen and liver are organs that respond directly to the presence of bacteria in the bloodstream, which enabled higher detection of MAP in these tissues. Interestingly, besides the spleen and liver, the colon also had significant proportion of positives. In intravenous inoculation in sheep, MAP was not recovered from gut-associated tissues, but in the spleen after 72h (Bower et al. 2013). However, the fact that the colon demonstrates the same probability of detection as the liver at 30 days of infection suggests that in some situations, MAP could have tropism for intestinal cells, even at early stages of an infection. In cattle experimentally infected via IP or orally, the ileum and associated lymph nodes were the organs with highest DNA detection and isolation of MAP (Sweeney et al. 2006, Stabel et al. 2009). In the present experimental model, ileum and Peyer's patches were not proportionally significant in detecting MAP-DNA in the first 90 days of infection. Despite parenchymal organs presenting proportionately higher positivity values compared to the ileum in all four evaluation periods, not been verified the absence of positives in these periods, for intestinal tissues. The evaluation of bovine tissue samples also did not verify the presence of MAP exclusively in parenchymal organs or in mesenteric lymph nodes (Pavlik et al. 2000). Further, after 30 days of oral inoculation, a greater amount of MAP was found in the C57BL/6 mice intestine compared with the liver and spleen (Bermudez et al. 2010). However, in the present work, the IP inoculation resulted in a systemic distribution of MAP, but did not lead to the detection of

MAP-DNA only in parenchymal organs (liver and spleen), confirming that MAP can be present in the intestine irrespective of the route of infection and when present in the bloodstream, it also has tropism for the colon, principally.

The assessments of odds ratio and RR in studies of paratuberculosis is usually related to the search for risk factors associated with management practices applied to livestock and the prior presence of the disease among herds (Kobayashi et al. 2007, Ansari-Lari et al. 2009), but not correlated with the probability of organs to be positive according to the time post-inoculation. In suspected herds, the necropsy of certain animals and the identification of a specific organ with a higher risk of being positive relative to others during infections stages are important to assist in the early detection of infected animals in the herd, but also in experimental models, to understand the behavior of the microorganism during an infection. Among the associations between the organs, it was observed that samples of spleen have a higher risk of confirming an infection, especially when compared to samples of the ileum and Peyer's patches (Table 3). In part, this can be explained by the degree of blood perfusion in the organs, where once the microorganism reaches the bloodstream, tissues with higher blood perfusion tend to have higher risk of being positives. Furthermore, the greatest expressions of IFN-γ found in the liver and spleen (Fig.2A,B) suggest that these organs are also possibly responsible for this cytokine to increase peripheral blood since early stage of infection. Increased expression of this cytokine has been reported in mononuclear cells from peripheral blood of cattle infected with MAP, correlating these levels in the early stage or subclinical infection in both natural or experimental infection (Stabel 2000, Coussens et al. 2003, Waters et al. 2003, Khalifeh & Stabel 2004).

The formation of granulomas at the site of mycobacterial infection is a direct response of host immunity. Among the factors responsible for this formation, TNF-α plays an important role in host resistance against mycobacterial infection. We found that the ileum was shown to be the main tissue responsible for synthesizing TNF-α from at 60th day (Fig.2C). Normally, the expression of IFN-γ, TNF-α, and IL-2 is present in the cell-mediated immune response, in the initial stage of paratuberculosis (Burrells et al. 1999, Stabel 2000). However, previous studies have shown that the expression of TNF-α transcript in the ileum did not appear to be affected by infection with MAP because it was not possible to establish a statistical significant difference in the samples (Lee et al. 2001, Tanaka et al. 2005, Robinson et al. 2011). Nevertheless, we found that the expression of TNF-α in the ileum was significantly affected by MAP infection in this organ (Fig.2C). Thus, these results may help to explain the diffuse nature of granulomas at sites of infection, since TNF-α is required for suitable formation of well-defined granulomas (Ehlers et al. 2000, Roach et al. 2002). Although it has been reported that IL-4 expression occurs in clinical stages of infection (Tanaka et al. 2005), significantly higher levels of IL-4 were obtained at 60 days compared to 30 days in the ileum (Fig.2D). Robinson et al. (2011) found significantly lower expression of IL-4 when examining lymph nodes of the jejunum of severely ill deer

compared to minimally ill and negative control animals. Thus, our results suggest that IL-4 can be expressed in specifics stages of experimental infection, but further studies should be conducted to verify its action concurrently with the production of pro inflammatory cytokines in natural infections. Similar to IL-4, IL-10 is also synthesized at sites of MAP infection and is related to the progression of clinical paratuberculosis, being expressed mainly in the lymph node of the ileum of animals with multibacillary lesions (Tanaka et al. 2005, Smeed et al. 2007). Even though it is not significant, the expression of IL-10 in the colon at 90 days indicates that this cytokine, as well as IL-4, may be present in high quantities in later stages of infection in mice that did not present lesions.

The results presented in this study contribute to a better understanding of the mainly organs that are infected by MAP during an IP infection and will support in future experiments that uses mice as model for MAP infection. Furthermore, enabled to understand which cytokines are more expressed in specific organs during experimental infection with MAP, assisting in the understanding of immunopathogenesis of MAP and future diagnostic tests for early detection of infection.

CONCLUSIONS

For molecular detection of MAP, spleen, colon and liver proved to be the best organs to confirm the experimental infection in C54BL/6 mice.

Sixty days post-infection was the crucial time for detecting the expression IFN-γ by the spleen and liver; and TNF-α and IL-4 by the ileum.

REFERENCES

Allen A.J., Park K.T., Barrington G.M., Lahmers K.K., Abdellrazeq G.S., Rihan H.M., Sreevatsan S., Davies C., Hamilton M.J. & Davis W.C. 2011. Experimental infection of a bovine model with human isolates of *Mycobacterium avium* subsp. *paratuberculosis.* Vet. Immun. Immunopathol. 141:258-266.

Ansari-Lari M., Haghkhah M., Bahramy A. & Novin Baheran A.M. 2009. Risk factors for *Mycobacterium avium* subspecies *paratuberculosis* in fars province (Southern Iran) dairy herds. Trop. Anim. Health Prod. 41:553-557.

Bermudez L.E., Petrofsky M., Sommer S. & Barletta R.G. 2010. Peyer's patch-deficient mice demonstrate that *Mycobacterium avium* subsp. *paratuberculosis* translocates across the mucosal barrier via both M cells and enterocytes but has inefficient dissemination. Infect. Immun. 78:3570-3577.

Bower K.L., Begg D.J. & Whittington R.J. 2013. Tissue localisation of *Mycobacterium avium* subspecies *paratuberculosis* following artificially induced intracellular and naked bacteraemia. Vet. Microbiol. 162:112-118.

Burrells C., Clarke C.J., Colston A., Kay J.M., Porter J., Little D. & Sharp J.M. 1999. Interferon- gamma and interleukin-2 release by lymphocytes derived from the blood, mesenteric lymph nodes and intestines of normal sheep and those affected with paratuberculosis (Johne's disease). Vet. Immunol. Immunopathol. 68:139-148.

Carvalho I.A., Silva V.O., Vidigal P.M.P., Silva Júnior A. & Moreira M.A.S. 2012. Genetic evaluation of IS900 partial sequence of *Mycobacterium avium* subsp. *paratuberculosis* Brazilian isolates from bovine milk. Trop. Anim. Health Prod. 44:1331-1334.

Chen L.H., Kathaperumal K., Huang C.J., McDonough S.P., Stehman S., Akey B., Huntley J., Bannantine J.P., Chang C.F. & Chang Y.F. 2008. Immune responses in mice to *Mycobacterium avium* subsp. *paratuberculosis* following vaccination with a novel 74F recombinant polyprotein. Vaccine 26:1253-1262.

Chiodini R.J. & Buergelt C.D. 1993. Susceptibility of Balb/c, C57/B6 and C57/B10 mice to infection with *Mycobacterium paratuberculosis*. J. Comp. Pathol. 109:309-319.

Chiodini R.J., Van Kruiningen H.J. & Merkal R.S. 1984. Ruminant paratuberculosis (Johne's disease): the current status and future prospects. Cornell Vet. 74:218-262.

Clarke C.J. 1997. Paratuberculosis and molecular biology. Vet. J. 153:245-247.

Coussens P.M., Colvin C.J., Wiersma K., Abouzied A. & Sipkovsky S. 2002. Gene expression profiling of peripheral blood mononuclear cells from cattle infected with *Mycobacterium paratuberculosis*. Infect. Immun. 70:5494-5502.

Coussens P.M., Colvin C.J., Rosa G.J., Perez L.J. & Elftman M.D. 2003. Evidence for a novel gene expression program in peripheral blood mononuclear cells from *Mycobacterium avium* subsp. *paratuberculosis*-infected cattle. Infect Immun. 71:6487–6498.

Coussens P.M., Verman N., Coussens M.A., Elftman M.D. & McNulty A.M. 2004. Cytokine gene expression in peripheral blood mononuclear cells and tissues of cattle infected with *Mycobacterium avium* subsp. *paratuberculosis*: evidence for an inherent proinflamatory gene expression pattern. Infect. Immun. 72:1409-1422.

Ehlers S., Kutsch S., Ehlers E.M., Benini J. & Pfeffer K. 2000. Lethal granuloma disintegration in mycobacteria-infected TNFRp55/mice is dependent on T cells and IL-12. J. Immunol. 165:483-492.

Englund S., Ballagi-Pordány A., Bölske G. & Johansson K. 1999. Single PCR and nested PCR with a mimic molecule for detection of *Mycobacterium avium* subsp. *paratuberculosis*. Diagn. Microb. Infect. Dis. 33:163-171.

Harris N.B. & Barleta R.G. 2001. *Mycobacterium avium* subsp. *paratuberculosis* in veterinary medicine. Clin. Microbiol. Rev. 14:489-512.

Khalifeh M.S. & Stabel J.R. 2004. Effects of gamma interferon, interleukin-10, and transforming growth factor beta on the survival of *Mycobacterium avium* subsp. *paratuberculosis* in monocyte-derived macrophages from naturally infected cattle. Infect. Immun. 72:1974-1982.

Kobayashi S., Tsutsui T., Yamamoto T. & Nishiguchi A. 2007. Epidemiologic indicators associated with within-farm spread of Johne's disease in dairy farms in Japan. J. Vet. Med. Sci. 69:1255-1258.

Koo H.C., Park Y.H., Hamilton M.J., Barrington G.M., Davies C.J., Kim J.B., Dahl J.L., Waters W.R. & Davis W.C. 2004. Analysis of the immune response to *Mycobacterium avium* subsp. *paratuberculosis* in experimentally infected calves. Infect. Immun. 72:6870-6883.

Lee H., Stabel J.R. & Kehrli Jr M.E. 2001. Cytokine gene expression in ileal tissues of cattle infected with *Mycobacterium paratuberculosis*. Vet. Immunol. Immunopatholo. 82:73-85.

Livak K.J. & Schmittgen T.D. 2001. Analysis of relative gene expression data using real-time quantitative PCR and the 2(-Delta Delta C(T)). Method. Methods 25:402-408.

Mendoza J.L., Lana R. & Diaz-Rubio M. 2009. *Mycobacterium avium* subspecies *paratuberculosis* and its relationship with Crohn's disease. World J. Gastroenterol. 15:417-422.

Mutwiri G.K., Butler D.G., Rosendal S. & Yager J. 1992. Experimental infection of severe combined immunodeficient beige mice with *Mycobacterium paratuberculosis* of bovine origin. Infect. Immun. 60:4074-4079.

Park S.U., Kathaperumal K., McDonough S., Akey B., Huntley J., Bannantine J.P. & Chang Y.F. 2008. Immunization with a DNA vaccine cocktail induces a Th1 response and protects mice against *Mycobacterium avium* subsp. *paratuberculosis* challenge. Vaccine 26:4329-4337.

Pavlik I., Matlova L., Bartl J., Svastova P., Dvorska L. & Whitlock R. 2000. Parallel faecal and organ *Mycobacterium avium* subsp. *paratuberculosis* culture of different productivity types of cattle. Vet. Microbiol. 77:309-324.

Roach D.R., Bean A.G., Demangel C., France M.P., Briscoe H. & Britton W.J. 2002. TNF regulates chemokine induction essential for cell recruitment, granuloma formation, and clearance of mycobacterial infection. J. Immunol. 168:4620-4627.

Robinson M.W., O'brien R., Mackintosh C.G., Clark R.G. & Griffin J.F. 2011. Immunoregulatory cytokines are associated with protection from immunopathology following *Mycobacterium avium* subspecies *paratuberculosis* infection in red deer. Infect. Immun. 79:2089-2097.

Roupie V., Rosseels V., Piersoel V., Zinniel D.K., Barletta R.G. & Huygen K. 2008. Genetic resistance of mice to *Mycobacterium paratuberculosis* is influenced by Slc11a1 at the early but not at the late stage of infection. Infect. Immun. 76:2099-2105.

Sivakumar P., Tripathi B.N. & Singh N. 2005. Detection of *Mycobacterium avium* subsp. *paratuberculosis* in intestinal and lymph node tissues of water buffaloes (*Bubalus bubalis*) by PCR and bacterial culture. Vet. Microbiol. 108:263-270.

Smeed J.A., Watkins C.A., Rhind S.M. & Hopkins J. 2007. Differential cytokine gene expression profiles in the three pathological forms of sheep paratuberculosis. BMC Vet. Res. 3:18-28.

Stabel J.R. 2000. Cytokine secretion by peripheral blood mononuclear cells from cows infected with *Mycobacterium paratuberculosis*. Am. J. Vet. Res. 61:754-760.

Stabel J.R., Palmer M.V., Harris B., Plattner B., Hostetter J. & Robbe-Austerman S. 2009. Pathogenesis of *Mycobacterium avium* subsp. *paratuberculosis* in neonatal calves after oral or intraperitoneal experimental infection. Vet. Microbiol. 136:306-313.

Sweeney R.W., Uzonna J., Whitlock R.H., Habecker P.L., Chilton P. & Scott P. 2006. Tissue predilection sites and effect of dose on *Mycobacterium avium* subs. *paratuberculosis* organism recovery in a short-term bovine experimental oral infection model. Res. Vet. Sci. 80:253-259.

Tanaka S., Sato M., Onitsuka T., Kamata H. & Yokomizo Y. 2005. Inflammatory cytokine gene expression in different types of granulomatous lesions during asymptomatic stages of bovine paratuberculosis. Vet. Pathol. 42:579-588.

Verna A.E., Garcia-Pariente C., Munoz M., Moreno O., Garcia-Marin J.F., Romano M.I., Paolicchi F. & Perez V. 2007. Variation in the immuno-pathological responses of lambs after experimental infection with different strains of *Mycobacterium avium* subsp. *paratuberculosis*. Zoonoses Public Health 54:243-252.

Waters W.R., Miller J.M., Palmer M.V., Stabel J.R., Jones D.E., Koistinen K.A., Steadham E.M., Hamilton M.J., Davis W.C. & Bannantine J.P. 2003. Early induction of humoral and cellular immune responses during experimental *Mycobacterium avium* subsp. *paratuberculosis* infection of calves. Infect. Immun. 71:5130-5238.

Yao X., Tan Z., Gu B., Wu R., Liu Y., Dai L. & Zhang M. 2010. Promotion of self-renewal of embryonic stem cells by midkine. Acta Pharm. Sini. 31:629-637.